ESC European Society of Cardiology

European Heart Journal - Cardiovascular Imaging (2023) **24**, 78–87
https://doi.org/10.1093/ehjci/jeab294

**ORIGINAL PAPER**

# Cardiovascular magnetic resonance-derived *left ventricular* intraventricular pressure gradients among patients with precapillary pulmonary hypertension

**Jacqueline L. Vos [1], Tim Leiner [2,3], Arie P.J. van Dijk[1], Gianni Pedrizzetti[4], Fawaz Alenezi[5], Laura Rodwell[6], Constantijn T.P.M. van der Wegen[1], Marco C. Post[7], Mieke M.P. Driessen[1,2], and Robin Nijveldt [1]***

[1]Department of Cardiology, Radboud University Medical Center, Geert Grooteplein 10, 6525 GA Nijmegen, The Netherlands; [2]Department of Radiology, Mayo Clinic, Rochester, MN, USA; [3]Department of Radiology, University Medical Center Utrecht, Utrecht, The Netherlands; [4]Department of Engineering and Architecture, University of Trieste, Trieste, Italy; [5]Department of Cardiology, Duke Heart Center, Durham, NC, USA; [6]Department of Health Sciences, section Biostatistics, Radboud Institute for Health Sciences, Nijmegen, the Netherlands; and [7]Department of Cardiology, St. Antonius, Nieuwegein, The Netherlands

*Received 6 August 2021; editorial decision 20 December 2021; accepted 22 December 2021; online publish-ahead-of-print 5 January 2022*

**Aims** Precapillary pulmonary hypertension (pPH) affects left ventricular (LV) function by ventricular interdependence. Since LV ejection fraction (EF) is commonly preserved, LV dysfunction should be assessed with more sensitive techniques. Left atrial (LA) strain and estimation of LV intraventricular pressure gradients (IVPG) may be valuable in detecting subtle changes in LV mechanics; however, the value of these techniques in pPH is unknown. Therefore, the aim of our study is to evaluate LA strain and LV-IVPGs from cardiovascular magnetic resonance (CMR) cines in pPH patients.

**Methods and results** In this cross-sectional study, 31 pPH patients and 22 healthy volunteers underwent CMR imaging. Feature-tracking LA strain was measured on four- and two-chamber cines. LV-IVPGs (from apex–base) are computed from a formulation using the myocardial movement and velocity of the reconstructed 3D-LV (derived from long-axis cines using feature-tracking). Systolic function, both LV EF and systolic ejection IVPG, was preserved in pPH patients. Compared to healthy volunteers, diastolic function was impaired in pPH patients, depicted by (i) lower LA reservoir ($36 \pm 7\%$ vs. $26 \pm 9\%$, $P < 0.001$) and conduit strain ($26 \pm 6\%$ vs. $15 \pm 8\%$, $P < 0.001$) and (ii) impaired diastolic suction ($-9.1 \pm 3.0$ vs. $-6.4 \pm 4.4$, $P = 0.02$) and E-wave decelerative IVPG ($8.9 \pm 2.6$ vs. $5.7 \pm 3.1$, $P < 0.001$). Additionally, 11 pPH patients (35%) showed reversal of IVPG at systolic–diastolic transition compared to none of the healthy volunteers ($P = 0.002$).

**Conclusions** pPH impacts LV function by altering diastolic function, demonstrated by an impairment of LA phasic function and LV-IVPG analysis. These parameters could therefore potentially be used as early markers for LV functional decline in pPH patients.



* Corresponding author. Tel: +31 24 3616785; Fax: +31 24 3635111. E-mail: robin.nijveldt@radboudumc.nl

## Graphical Abstract

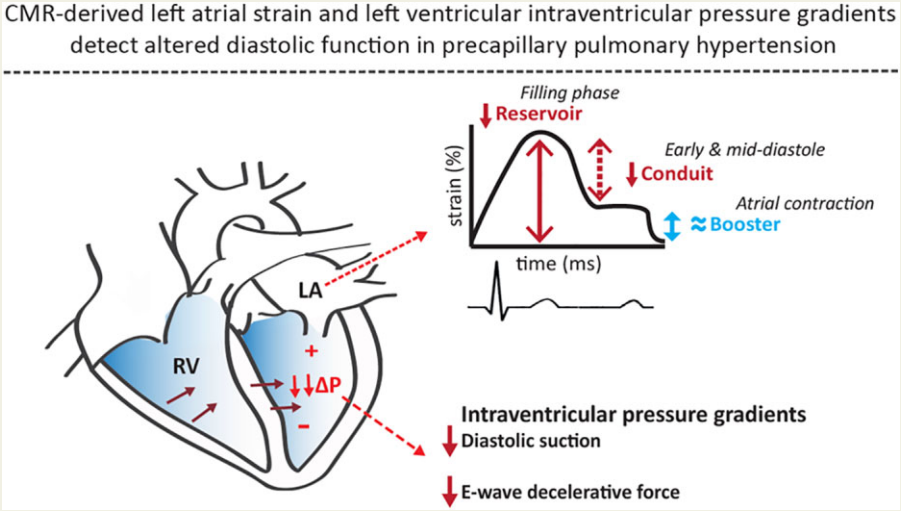


**Keywords** pulmonary hypertension • CMR • feature tracking • left ventricular strain • left atrial strain • intraventricular pressure gradient

# Introduction

In precapillary pulmonary hypertension (pPH) the right ventricular (RV) afterload is increased, inducing RV adaptation, such as increased RV contractility and hypertrophy. Ultimately, when adaptation falls short, the RV dilates and function deteriorates.[1] Simultaneously, pPH also affects left ventricular (LV) function by ventricular interdependence; however, the pathophysiological mechanism is not completely elucidated. In addition, since LV ejection fraction (EF) is often in the normal range, these LV alterations are difficult to recognize and often overlooked, although signs of diastolic dysfunction on echocardiography is quite common in pPH.[2] This is unfavourable, since recent research showed that impaired LV strain is associated with worse outcomes,[3,4] stressing the importance of comprehensive assessment of LV function in pPH.

There is increasing interest in intraventricular pressure gradients (IVPGs) patterns, driving cardiac blood flow. It is thought that abnormalities in IVPGs precede cardiac remodelling, and may therefore be a potential marker of preclinical disease.[5] In the past, IVPGs have shown interesting alterations in heart failure and myocardial ischaemia.[6–8] However, measurement of IVPGs has never made it to daily clinical practice, due to the difficulty and invasive character. A novel method, based on the same principle, has recently been described, which makes it possible to estimate IVPGs non-invasively from routinely obtained cardiovascular magnetic resonance (CMR) cine images.[9] This approach has shown promising results in heart failure patients, showing impaired LV IVPGs in heart failure with preserved LVEF.[10] Besides IVPG analysis, other promising parameters have emerged, such as CMR-feature tracking LV strain and left atrial (LA) phasic function,[11] providing additional insight in LV function. The latter is of special interest, since alterations in LA phasic function correlate with LV end-diastolic pressure, and are found to precede overt heart failure.[12]

In summary, alterations in LA phasic strain and IVPGs can potentially help our understanding of the pathophysiological mechanism of ventricular interdependence in pPH patients, and might have the ability to identify alterations in LV function at an early stage. Therefore, the aim of our study is to evaluate CMR-derived LA phasic function and LV IVPGs in pPH patients in comparison to healthy volunteers.

# Methods

In this cross-sectional study, pPH patients and healthy volunteers (aged 30–60 years, $n = 22$) were enrolled between August 2012 and November 2013.[13] pPH (idiopathic pulmonary arterial hypertension or chronic thromboembolic PH) was previously established by pulmonary arterial pressure ≥25 mmHg at rest and a pulmonary capillary wedge ≤15 mmHg measured during right heart catheterization, in accordance with the European Society of Cardiology/European Respiratory Society (ESC/ERS) guidelines.[14] Patients were clinically stable on their last visit, without overt clinical heart failure. Patients were recruited from three tertiary hospitals in The Netherlands. All study participants underwent a transthoracic echocardiogram (TTE) and CMR on the same day, and demographic data were collected. Study participants were excluded in case of insufficient quality of more than one CMR long-axis cines (two-, three-, or four-chamber). The Ethical Review boards of all participating centres approved the study. Written informed consent was obtained from all study participants prior to inclusion.

## Echocardiography acquisition

TTE was performed using a Toshiba Artida system (Toshiba Medical Systems, Tokyo, Japan) with a 5-MHz transducer in all study participants, and offline analysis was performed on commercially available software (XCelera, version 4.1.1.1133-2013; Philips Healthcare, Best, The Netherlands). Transmitral flow, using pulsed wave Doppler-imaging at the mitral leaflet tips in the apical four-chamber view, was used to measure early (*E*) and late/atrial (*A*) velocities. Pulsed-wave tissue Doppler was used to measure early diastolic velocities at the lateral and septal mitral annulus (e′ lateral and e′ septal). E/A ratios and *E*/e′ septal and *E*/e′ lateral ratios were calculated.[15] RV systolic pressure (RVSP) was calculated by adding the estimated right atrial pressure to the pressure gradient derived from the Bernoulli equation using the peak velocity of the tricuspid regurgitation.[16] The TAPSE/RVSP ratio was calculated as a marker of ventricular–pulmonary arterial coupling.[17]

## CMR acquisition

All study participants were scanned on a commercially available 1.5 T CMR scanner (Ingenia R4.1.2; Philips healthcare, Best, The Netherlands). Balanced steady-state free-precession (long- and short-axis) cine images were acquired during end-expiratory breath holds, with the following sequence parameters: TR/TE 3.4/1.69 ms, voxel size 1.3 × 1.3 × 8.0 mm, flip angle of 55°, and 30 phases per cardiac cycle. The consecutive short-axis cine images from base to apex were used to analyse RV and LV mass, volumes, and calculate EF.

## Interventricular septal angle measurement

To evaluate the deformation of the septum due to RV enlargement and pressure overload, the interventricular septal angle was measured on the midventricular short-axis cine at the phase of maximum septal displacement. The septal angle was defined as the angle between the RV insertion points and the septal midpoint. The interventricular septal angle ratio is calculated by dividing the interventricular septal angle by the angle of the free wall.[18,19]

## CMR feature tracking analysis

LV global longitudinal strain (GLS) was measured on the long-axis cine images (two-, three-, and four-chamber cine images) using Medis QStrain software (Medis Medical Imaging BV, version 2.0.48.8., Leiden, The Netherlands). Endocardial contours were manually drawn in the end-systolic and end-diastolic frame, after which the software automatically tracks endocardial contours in all other consecutive frames and calculates the myocardial shortening throughout the cardiac cycle. The automatically drawn contours were checked carefully, and manually adjusted when needed. LA phasic strain was measured on the two-, and four-chamber cine images, and the LA reservoir (collecting pulmonary venous return during LV systole), conduit (deflecting the early- and mid-diastole; the passive filling of blood from LA to LV), and booster strain (deflecting the active, late diastole; the atrial kick) were measured. Using the biplane Simpson's area-length method, LA volumes and EF were automatically calculated by QStrain.[20]

## CMR LV-IVPG analysis

LV-IVPGs are computed from a formulation using the myocardial movement and velocity of the reconstructed 3D-LV (derived from the long-axis cines using feature-tracking), and the amount of blood crossing the valves (conservation of mass principle). The diameters of the mitral valve and aortic valve are manually drawn, and the outflow area is calculated by QStrain software. The volume integral of IVPGs is a force and has the dimension of Newton, it is normalized for LV volume and divided by the specific gravity of blood to make it a dimensionless measure, which can be interpreted as a % of force of gravity. The apex to base IVPG is the principal component of the IVPG vector, its time curve is generated by the software and represents the variation of IVPG throughout the cardiac cycle. LV contraction creates the systolic ejection phase 'the A-wave', a positive IVPG directed from apex to base (LV outflow tract). The systolic–diastolic transition 'the B-wave' is a negative IVPG wave from apex to base, and starts during the final phase of systole (aortic valve open), contains the isovolumic relaxation phase and terminates after the initial impulsive phase of diastolic early filling (mitral valve open). B1 is when the LV contraction slows-down, and ends when the LV relaxes and unwinds, closing the aortic valve and eventually lowering LV pressure below the LA pressure. This is followed by mitral valve opening, and the negative IVPG from apex–base leads to an acceleration of blood flow in the first phase of LV filling (diastolic suction) in early diastole, called 'B2'. The slowing blood flow rate at the end of the passive LV filling phase represents the E-wave decelerative force (C-wave; a positive IVPG from apex to base), until the pressure gradient equilibrates (diastasis). Next, LA contraction drives a second negative pressure gradient (active, late diastole) from apex to base[21]; the A-wave acceleration (the D-wave). The A-, B- (B1 and B2), C-, and D-waves are measured by manually marking the different phases (using the IVPG pattern, the volume-curve and valvular opening and closing). The IVPG curve and corresponding phases in the healthy situation are illustrated in *Figure 1*, and a tutorial video of the IVPG analysis with an IVPG curve of a healthy volunteer, and one of a pPH patient can be found in the Supplementary data online, *Video S1*. All strain and IVPG analyses were performed by one single investigator (J.L.V.), supervised by a level III CMR-physician with >15 years of experience (R.N.).

## Statistical analysis

Continuous variables are presented as mean ± standard deviation (if normally distributed) or median (inter-quartile range) if not normally distributed. Categorical variables are presented as total number (percentage). Precapillary PH patients and the control group are compared for continuous variables using the independent sample *t*-test or Mann–Whitney *U*. The $\chi^2$ test or the Fisher's exact test was used to compare categorical variables between groups. Since the healthy volunteers were not age- and sex-matched, the independent influence of pPH on the CMR parameters (interventricular septal angle, strain, and IVPG analysis) was determined by performing a multiple linear regression analysis with adjustment for sex and age. To evaluate the correlation between the strain and IVPG analysis with established echocardiographic diastolic markers, and the correlation with markers of pPH severity (TR velocity, TAPSE/RVSP ratio, and interventricular septal angle on CMR), a Pearson correlation coefficient *R* was calculated. To evaluate intra- and interoberserver variability of the IVPG analysis, and interventricular septal angle and ratio, analyses were repeated in 15 CMR scans by one single investigator (J.L.V., >2 weeks after the first analysis) and two investigators (J.L.V. and C.T.P.M.v.d.W.), respectively. The intraclass correlation coefficient was used to measure inter- and intraobserver variability. All statistical analyses were performed using SPSS (version 25). A *P*-value <0.05 was considered statistically significant.

# Results

## Study population

Of the 33 consecutive enrolled pPH patients, 2 pPH patients were excluded due to insufficient CMR cine quality. In total, 31 pPH patients [aged 54 (45–62) years, 29% male] and 22 healthy volunteers [aged 40 (36–48) years, 68% male] were included in this study.

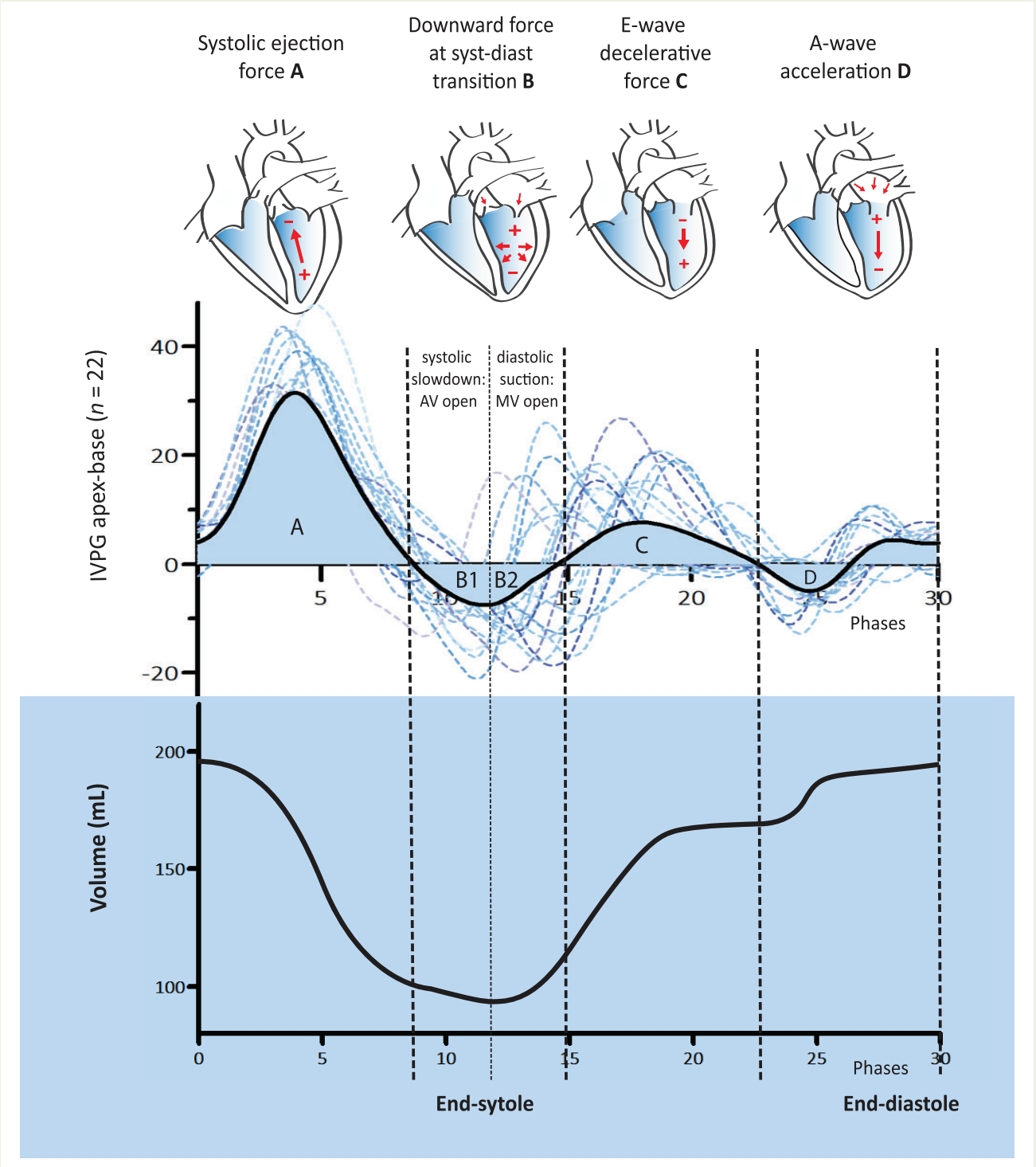


**Figure 1** The apex–base time curve of left ventricular intraventricular pressure gradients. Depiction of the LV-IVPGs from apex to base (*y*-axis) in time (ms, *x*-axis) in healthy volunteers ($n = 22$), with corresponding volume curve (bottom graph). The coloured dotted lines are IVPG curves of individual healthy volunteers, the solid black line represents the average. The positive IVPG to base (LV outflow tract), created by LV contraction, is the systolic ejection phase 'A'. Second, a negative IVPG wave (apex–base) takes place in the downward force at systolic–diastolic transition 'B', created by the relaxation and unwinding of the LV, lowering LV pressure below aortic pressure leading to aortic valve closure 'B1', and eventually below LA pressure causing the opening of the mitral valve. This leads to an acceleration of blood flow in the first phase of passive LV filling (suction) in early diastole 'B2'. Third, a positive IVPG (apex–base) is created by the slowing blood flow rate at the end of the passive LV filling phase, represented by the E-wave decelerative force 'C', until pressure gradient equilibrates (diastasis). Lastly, LA contraction drives a second negative IVPG (apex–base) in the active, late diastole, depicted by the A-wave acceleration 'D'. AV, aortic valve; IVPG, intraventricular pressure gradient analysis; LA, left atrial; LV, left ventricular; MV, mitral valve; syst–diast, systolic–diastolic.

Healthy volunteers were younger ($P = 0.003$) and a larger proportion was male ($P = 0.005$). Fifteen pPH patients (48%) were diagnosed with chronic thromboembolic pulmonary hypertension, and 16 (52%) were diagnosed with idiopathic pulmonary arterial hypertension. Mean duration of disease was 4.7 ± 2.8 years. Most pPH patients received mono- (39%) or dual (48%) PH-specific treatment, and had a WHO functional class of II (68%) or III (26%). The specific details are displayed in Supplementary data online, *Table S1*.

## Baseline echocardiographic and CMR parameters

*Table 1* shows echocardiographic and CMR findings. The mean tricuspid regurgitation velocity was 3.6 ± 0.7 m/s in pPH patients. The TAPSE/RVSP ratio, a measure of RV-pulmonary arterial coupling, was lower in pPH. Compared to healthy volunteers, peak A velocity was higher in pPH patients, whereas peak E velocity was similar, resulting in a lower E/A ratio. Compared to healthy volunteers, pPH patients had lower $e'$ lateral and septal velocity, and $E/e'$ septal ratio was higher.

CMR-derived LV end-diastolic and end-systolic volumes were lower in pPH patients than in healthy volunteers, whereas LVEF was similar (*Table 1*). pPH patients had higher RV end-diastolic volumes and RV end-systolic volumes, and RVEF was lower. LA EF was lower in pPH patients compared to healthy volunteers.

The interventricular septal angle was higher in pPH patients, with subsequently a higher interventricular septal angle ratio, meaning higher septal deviation towards the left ventricle than in healthy volunteers. Additionally, there was a strong correlation between the interventricular septal angle and echocardiographic estimates of RV pressure (Pearson's $R = 0.70$ for TR velocity and 0.86 for RVSP, $P < 0.001$ for both).

## Diastolic CMR-derived strain and IVPG analysis are worse in pPH patients

Compared to healthy volunteers, both LA reservoir and conduit strain were impaired in pPH patients (*Table 2*), LA booster strain was similar (10 ± 5% vs. 11 ± 4%, $P = 0.35$). LV longitudinal strain analysis was also impaired in pPH patients compared to healthy volunteers. pPH remained independently associated with LA reservoir and conduit strain after adjustment for age and sex, whereas LV strain did not (Supplementary data online, *Table S2*).

Systolic function estimated by the IVPG systolic ejection force 'A' did not show any significant alteration between healthy volunteers and pPH patients (*Table 2*) and was even associated with higher values of force when adjusted for age and sex (Supplementary data online, *Table S2*). Contrarily, IVPG analysis showed impaired diastolic function. In the early and mid-diastolic passive filling phase, pPH patients had impaired diastolic suction force 'B2' and E-wave decelerative force 'C' compared to healthy controls (*Table 2*), independent of sex and age (Supplementary data online, *Table S2*). In addition, 11 pPH patients (35%) had reversal of IVPG at systolic-diastolic transition 'B', whereas none of the healthy volunteers showed this pattern ($P = 0.002$). Especially the pPH patients with reversal in the diastolic suction force B2 ($n = 6$) had worse diastolic LV function and RV failure, more than pPH patients with reversal of IVPG in 'the systolic slowdown' B1 (n = 5). They had lower E velocity, $e'$ septal velocity, and $E/A$ ratio on echocardiography, higher RV volumes and worse RVEF, and a trend towards a worse interventricular septal angle, compared to pPH patients without reversal of IVPG in the B-wave (Supplementary data online, *Table S3*).

*Figure 2* shows LA strain and LV IVPG analysis in healthy volunteers and pPH patients. The IVPG curves of pPH patients are shown in *Figure 3*, illustrating preserved systolic ejection force A (consistent with the preserved LVEF), the reversal of IVPG at systolic–diastolic transition 'B' in one-third of the pPH patients, and the diminished diastolic suction force 'B2' and E-wave decelerative force 'C' in pPH patients.

## LA strain and LV-IVPG in relation to measures of diastolic dysfunction and pPH severity

Since LA strain and IVPG are new measures of diastolic dysfunction, we evaluated its relation with known parameters of diastolic function on echocardiography (*Table 3*). Both $E/A$ ratio and $e'$ lateral velocity were significantly correlated with LA reservoir and conduit strain, and the IVPG analysis of the 'B2' and 'C' wave (weak to moderate correlations, $P < 0.05$ for all). This was similar for $e'$ septal velocity. In addition, IVPG analyses ('B2' and 'C' wave) were significantly correlated with E velocity.

To evaluate whether the severity of pPH is linked to LV diastolic dysfunction, the association between measurements of pPH severity and ventricular interdependence (such as the TR velocity and the interventricular septal angle) and LA strain/IVPG were analysed (*Table 4*). Interestingly, there were significant weak to moderate correlations between LA strain/IVPG and measurements of pPH severity and interventricular interdependence ($P < 0.05$ for all).

## Reproducibility of IVPG analysis

The inter- and intraobserver variabilities were good to excellent for the interventricular septal angle and ratio, and all LV-IVPG measurements (intraclass correlation coefficients ranging from 0.75 to 0.99, Supplementary data online, *Table S4*).

# Discussion

This study is the first to non-invasively measure and analyse LV-IVPGs and LA strain for the evaluation of LV systolic and diastolic function in pPH patients in comparison to healthy volunteers. IVPG analysis shows that, although systolic function is preserved, pPH primarily impacts LV function by altering diastolic function. This is demonstrated by an impaired apex-to-base diastolic suction and E-wave decelerative force in the early to mid-diastole, which leads to less passive filling. In one-third of patients, reversal of IVPG in the systolic–diastolic transition (B-wave) was present, meaning that LV pressure temporarily exceeds LA pressure. LA phasic function confirms the alterations seen in the IVPG analysis, showing reduced reservoir and conduit strain, reflecting less LA expansion from pulmonary venous return, and reduced passive filling of blood from LA to LV. Overall, pPH impacts LV function by impairing early diastolic filling (*Graphical Abstract*). LA phasic function and LV-IVPG parameters could therefore potentially be used as early markers for LV functional decline in pPH patients.

**Table 1 Echocardiography and CMR parameters of healthy volunteers and precapillary pulmonary hypertension patients**

| | Healthy volunteers ($n = 22$) | pPH patients ($n = 31$) | *P*-value |
|---|---|---|---|
| Echocardiography | | | |
| *E* velocity (m/s) | 0.64 (0.52–0.81) | 0.65 (0.53–0.74) | 0.70 |
| *A* velocity (m/s) | 0.45 (0.40–0.55) | 0.64 (0.56–0.72) | **<0.001** |
| *e′* lateral velocity (m/s) | 0.15 (0.13–0.18) | 0.13 (0.10–0.16) | 0.03 |
| *e′* septal velocity (m/s) | 0.11 (0.10–0.12) | 0.08 (0.07–0.11) | **0.001** |
| *E/A* ratio | 1.4 (1.2–1.6) | 0.9 (0.7–1.2) | <0.001 |
| *E/e′* (lateral) ratio | 4.4 (3.4–5.5) | 4.5 (4.0–5.8) | 0.38 |
| *E/e′* (septal) ratio | 5.9 (5.2–6.9) | 7.6 (5.9–10.0) | **0.001** |
| Tricuspid annular plane systolic excursion (mm) | 24 ± 3 | 20 ± 4 | **<0.001** |
| Tricuspid regurgitation velocity (m/s)[a] | 2.0 ± 0.3 ($n = 11$) | 3.6 ± 0.7 | **<0.001** |
| Estimated RVSP (mmHg)[a] | 19 ± 3 ($n = 11$) | 58 ± 21 | **<0.001** |
| TAPSE/RVSP ratio | 1.4 (1.0–1.6) | 0.4 (0.2–0.5) | **<0.001** |
| CMR | | | |
| Global ventricular parameters | | | |
| LV EDV (mL) | 182 ± 35 | 151 ± 39 | **0.005** |
| LV indexed EDV (mL/m$^2$) | 94 ± 16 | 79 ± 18 | **0.002** |
| LV ESV (mL) | 80 ± 17 | 67 ± 23 | **0.04** |
| LV indexed ESV (mL/m$^2$) | 41 ± 9 | 35 ± 12 | **0.04** |
| LVEF (%) | 56 ± 3 | 56 ± 8 | 0.83 |
| RV EDV (mL) | 200 (152–225) | 221 (184–280) | **0.04** |
| RV indexed EDV (mL/m$^2$) | 100 (86–108) | 110 (96–141) | **0.02** |
| RV ESV (mL) | 91 ± 25 | 154 ± 79 | **0.001** |
| RV indexed ESV (mL/m$^2$) | 47 ± 10 | 84 ± 52 | **0.002** |
| RVEF (%) | 55 ± 5 | 41 ± 12 | **<0.001** |
| RV mass (g) | 25 ± 7 | 39 ± 14 | **<0.001** |
| RV indexed mass (g/m$^2$) | 13 ± 3 | 21 ± 9 | **0.001** |
| Cardiac output (mL/min/kg/m$^2$) | 5.7 ± 1.2 | 5.4 ± 1.6 | 0.46 |
| Cardiac index (mL/min/kg/m$^2$) | 2.9 ± 0.4 | 2.8 ± 0.6 | 0.33 |
| Interventricular septal angle (°) | 127 ± 6 | 168 ± 21 | **<0.001** |
| Interventricular septal angle ratio | 1.8 ± 0.2 | 2.2 ± 0.2 | **<0.001** |
| Global left atrial parameters | | | |
| LA maximum volume (mL) | 107 (78–120) | 80 (67–116) | 0.20 |
| LA indexed maximum volume (mL/m$^2$) | 55 (45–61) | 44 (35–60) | 0.22 |
| LA minimum volume (mL) | 43 ± 17 | 46 ± 19 | 0.58 |
| LA indexed minimum volume (mL/m$^2$) | 22 ± 8 | 24 ± 10 | 0.48 |
| LA EF (%) | 59 ± 6 | 51 ± 9 | **<0.001** |

Values are in means ± SD, medians (interquartile range), or *n* (%). *P*-values <0.05 in bold.
CMR, cardiovascular magnetic resonance; EDV, end-diastolic volume; EF, ejection fraction; ESV, end-systolic volume; LA, left atrium; LV, left ventricular; pPH, precapillary pulmonary hypertension; RV, right ventricular; RVSP, right ventricular systolic pressure.
[a]Due to the lack of tricuspid regurgitation, this could not be measured in 11 healthy volunteers and 2 pPH patients.

Systolic LV function, usually measured by LVEF on echocardiography or CMR, is commonly preserved in pPH patients.[2,22] Therefore, the role of the left ventricle in this disease was often overlooked. Newer methods to analyse LV function, such as global LV strain, are able to detect more subtle and local changes, and exposed the impact of pPH on LV function and the association of LV functional decline with adverse prognosis.[2–4] In our study, LV strain was impaired in pPH patients compared to healthy volunteers. However, pPH was not independently associated with LV strain after adjustment for age and sex. Other studies did not find an impairment of global LV strain,[23] and it might be that LV strain, measuring myocardial shortening during systole, is not as sensitive for detecting early diastolic changes. In our study, the changes of IVPGs in different phases of the cardiac cycle show that systolic function is preserved, and that early diastolic filling is impaired. A weaker negative IVPG during the first part of the early diastolic filling ('B2' phase), results in lower inflow blood velocities, leading to lower deceleration of blood inflow during the second part of passive filling in pPH patients: a lower E-wave decelerative force 'C'. During systolic–diastolic transition, the LV relaxes and unwinds. In pPH, however, RV contraction is

**Table 2 CMR-derived strain and intraventricular pressure gradient analysis of healthy volunteers and precapillary pulmonary hypertension patients**

| | Healthy volunteers ($n = 22$) | pPH patients ($n = 31$) | *P*-value |
|---|---|---|---|
| Left atrial strain parameters | | | |
| Reservoir (%) | 36 ± 7 | 26 ± 9 | **<0.001** |
| Conduit (%) | 26 ± 6 | 15 ± 8 | **<0.001** |
| Booster (%) | 10 ± 5 | 11 ± 4 | 0.35 |
| Left ventricular strain parameters | | | |
| Global longitudinal strain (%) | -22 [-21 to -23] | -21 [-19 to -22] | **0.03** |
| Free wall longitudinal strain (%) | -23 [-21 to -25] | -25 [-23 to -26] | **0.02** |
| Septal longitudinal strain (%) | -20 [-17 to -21] | -17 [-15 to -20] | **0.08** |
| Intraventricular pressure gradient analysis (apex—base) | | | |
| Systolic ejection force 'A' | 16.8 ± 3.2 | 18.7 ± 5.4 | 0.14 |
| Downward force at systolic–diastolic transition 'B' | -7.4 ± 2.1 | -6.2 ± 2.3 | 0.28 |
| Reversal of force at systolic–diastolic transition 'B' | 0 | 11 (35%) | 0.002 |
| Diastolic suction force 'B2' | -9.1 ± 3.0 | -6.4 ± 4.4 | **0.02** |
| E-wave decelerative force 'C' | 8.9 ± 2.6 | 5.7 ± 3.1 | **<0.001** |
| A-wave Acceleration 'D' | -3.4 ± 1.8 | -3.0 ± 2.1 | 0.49 |

Values are in means ±SD, medians (interquartile range), or *n* (%). *P*-values <0.05 in bold.
CMR, cardiovascular magnetic resonance; pPH, precapillary pulmonary hypertension.

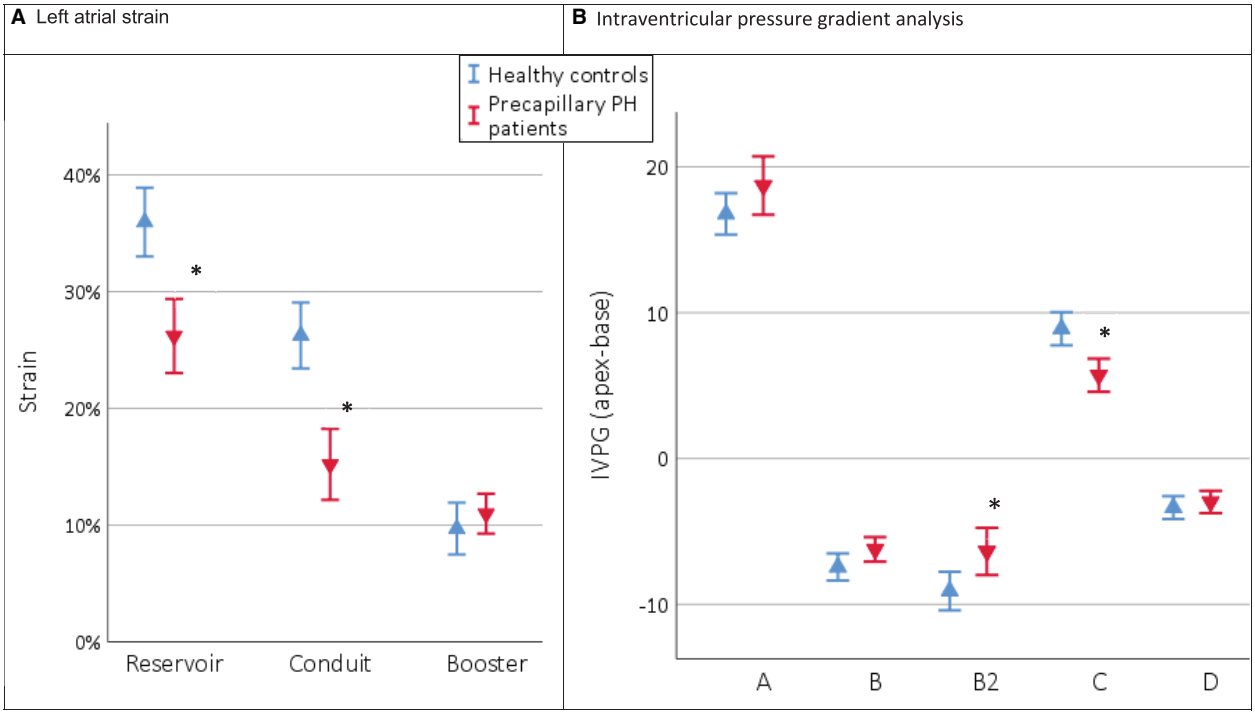


**Figure 2** Left atrial strain and left ventricular intraventricular pressure gradient analysis. (*A*) In pPH patients both left atrial reservoir and conduit strain were impaired compared to healthy volunteers. (*B*) The IVPG systolic ejection force 'A' did not show any significant alteration between healthy volunteers and pPH patients. In the early and mid-diastolic passive filling phase, pPH patients had impaired diastolic suction force 'B2' and E-wave decelerative force 'C' compared to healthy volunteers. Data are shown as mean values with 95% confidence interval. *$P < 0.05$. A, systolic ejection force 'A'; B, downward force at systolic–diastolic transition 'B'; 'B2', diastolic suction force 'B2'; C, E-wave decelerative force 'C'; D, A-wave acceleration 'D'; IVPG, Intraventricular pressure gradient; pPH, precapillary pulmonary hypertension.

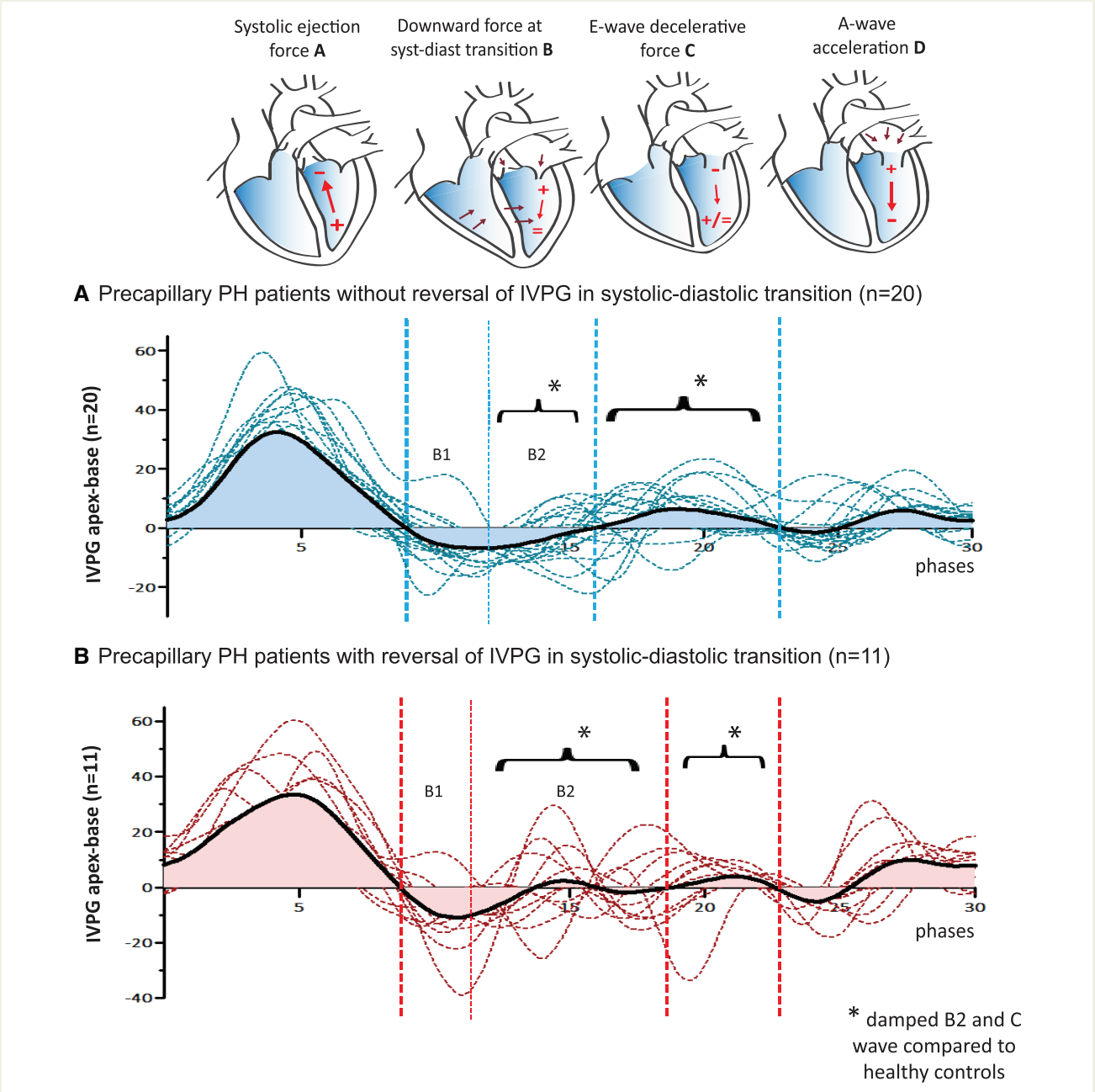


**Figure 3** Intraventricular pressure gradient analysis in precapillary pulmonary hypertension patients. Depiction of the LV IVPGs from apex to base (*y*-axis) in time (ms, *x*-axis). The coloured dotted lines are IVPG curves of individual patients, the solid black line the average curve in patients without (*A*, *n* = 20), and with reversal of IVPG in systolic–diastolic transition (*B*, *n* = 11). In the early diastolic phase, right after mitral valve opening, pPH patients had a weaker negative IVPG (apex–base) during diastolic suction force 'B2', resulting in lower inflow blood velocities. This leads to lower deceleration of blood inflow during the second part of passive filling: a lower E-wave decelerative force 'C'. One-third of pPH patients had reversal of IVPG at systolic–diastolic transition 'B' (pattern shown in B), whereas none of the healthy volunteers showed this pattern (*P* = 0.002). This is probably due to the prolonged RV contraction, which causes the septum to shift towards the LV, temporarily elevating the pressure gradient in the LV above the pressure in the LV base (LA), impairing early diastolic filling. IVPG, intraventricular pressure gradient analysis; LA, left atrial; LV, left ventricular; PH, pulmonary hypertension; syst–diast, systolic–diastolic.

prolonged, causing the septum to deviate towards the left, hindering LV inflow.[24] In our study, it even leads to reversal of the IVPG in one-third of pPH patients, which means that LV pressure temporarily surpasses the LA pressure. Next to the changes in LV-IVPGs, LA reservoir and conduit strain was impaired, confirming the alterations in diastolic filling in pPH patients compared to healthy volunteers. In the

**Table 3 Correlations of LA strain and LV-IVPG with markers of diastolic dysfunction on echocardiography**

| | e′ septal velocity | | e′ lateral velocity | | E velocity | | E/A ratio | |
|---|---|---|---|---|---|---|---|---|
| | *R* | *P*-value | *R* | *P*-value | *R* | *P*-value | *R* | *P*-value |
| Reservoir (%) | 0.36 | **0.009** | 0.45 | **0.001** | 0.18 | 0.2 | 0.38 | **0.005** |
| Conduit (%) | 0.47 | **<0.001** | 0.60 | **<0.001** | 0.19 | 0.17 | 0.47 | **<0.001** |
| Diastolic suction force 'B2' | –0.52 | **0.002** | -0.35 | **0.01** | -0.50 | **<0.001** | -0.33 | **0.01** |
| E-wave decelerative force 'C' | 0.62 | **<0.001** | 0.43 | **0.001** | 0.50 | **<0.001** | 0.56 | **<0.001** |

LA, left atrial; LV-IVPG, left ventricular intraventricular pressure gradients. *P*-values <0.05 in bold.

**Table 4 Correlations of LA strain and LV-IVPG with markers of pulmonary hypertension severity**

| | TR velocity | | TAPSE/RVSP ratio | | Indexed RV mass | | Intraventricular septal angle | |
|---|---|---|---|---|---|---|---|---|
| | *R* | *P*-value | *R* | *P*-value | *R* | *P*-value | *R* | *P*-value |
| LA reservoir strain (%) | –0.37 | **0.02** | 0.42 | **0.007** | -0.30 | **0.03** | -0.32 | **0.02** |
| LA conduit strain (%) | –0.56 | **<0.001** | 0.55 | **<0.001** | -0.44 | **0.001** | -0.44 | **0.001** |
| LV-IVPG diastolic suction force 'B2' | 0.33 | **0.04** | -0.31 | 0.06 | 0.40 | **0.003** | 0.36 | **0.009** |
| LV-IVPG E-wave decelative force 'C' | –0.44 | **0.005** | 0.47 | **0.003** | -0.41 | **0.002** | -0.46 | **<0.001** |

LA, left atrial; LV-IVPG, left ventricular intraventricular pressure gradient; TAPSE, tricuspid annular plane systolic excursion; TR, tricuspid regurgitation. *P*-values <0.05 in bold.

last decades, the LA has become a focus of interest in various diseases, since it is thought to reflect the severity of diastolic LV dysfunction,[25] and a recent echocardiographic study showed LA strain was a univariate predictor of mortality in severe pulmonary hypertension.[3]

The mechanism of diastolic dysfunction due to interventricular dependence in pPH is elegantly shown by Kasner *et al.*,[26] demonstrating that even mild pPH causes an increase in LV end-diastolic pressure, which was alleviated when RV filling was temporarily reduced (by vena cava inferior occlusion). The results of our study are in line with these findings. The interventricular septal angle, strongly associated with TR velocity and in previous research even to pulmonary arterial pressures on right heart catheterization,[19] correlated with LA strain and IVPG diastolic measurements. It is likely that diastolic dysfunction is not solely attributable to distortion of the LV chamber, but also to relative LV underfilling and low LV preload due to low right-sided cardiac output,[27] both resulting in lower LV end-diastolic and end-systolic volumes as is found in our study. The lower LA reservoir strain in pPH patients, which represents LA passive expansion of the pulmonary venous return, might reflect this lower LV preload.

The capability of CMR-derived-IVPG analysis to detect subtle alterations in diastolic function supports the theory that abnormalities in IVPG precede LV structural remodelling and might be a potential marker in preclinical disease. In addition, this method, validated against 4D flow CMR, the non-invasive gold standard for measuring blood velocities and calculating IVPGs,[28] and LA strain analysis use standard cine acquisitions and is not time-consuming (processing time between 7 and 10 min in total). These characteristics make the implementation of these analyses in daily clinical practice possible. The ability of detecting diastolic dysfunction in pPH patients by means of LV-IVPG or LA strain analysis is valuable, since some of the echocardiographic diagnostic criteria, such as the septal e′ velocity (which is influenced by the RV via interventricular interdependence), and RVSP cannot be used.[21] Future research is needed to evaluate whether these changes can guide prognosis or patient management. For example, in patients up for lung transplantation, since LV dysfunction is a common cause of morbidity after lung transplantation, and one of the most common causes of primary graft dysfunction.[29]

## Limitations

LA strain and LV-IVPG show promising results in this relatively small sized cohort study, however, these new techniques still have to be further evaluated in larger populations and in different cardiac diseases to see if these findings are consistent and reproducible. We only used the apex–base IVPG curve and not the inferolateral to anteroseptal IVPG curve, which might provide less consistent values.[28] We could not age and sex match the healthy volunteers to the pPH patients, however, age- and sex-adjusted analysis did not alter the results. Furthermore, since this CMR study is cross-sectional, it would be very interesting see how these IVPG patterns evolve over time, and to see whether these alterations are of prognostic or therapeutic importance in pPH patients.

# Conclusions

LA strain and LV-IVPG analysis show that pPH impacts LV function by altering diastolic function, demonstrated by impaired passive LV filling in the early- and mid-diastole. LA strain and LV-IVPG parameters could therefore potentially be used as early markers for LV functional decline in pPH patients.

# Supplementary data

Supplementary data are available at *European Heart Journal - Cardiovascular Imaging* online.

## Funding

Medis Suite Software (Medis Medical Imaging BV, version 2.0.48.8., Leiden, The Netherlands) has provided a license to analyse the IVPG on CMR. They had no role in the design and conduct of the study; collection, management, analysis, and interpretation of the data; preparation, review, or approval of the manuscript; and decision to submit the manuscript for publication. M.M.P.D. has received a research grant from the ICIN-Netherlands Heart House. R.N. received research grants from Biotronik and Philips.

**Conflict of interest:** none declared.

## Data availability statement

Original individual data are available upon reasonable request and can be obtained from the corresponding author.

## References

1. Vonk-Noordegraaf A, Haddad F, Chin KM, Forfia PR, Kawut SM, Lumens J *et al.* Right heart adaptation to pulmonary arterial hypertension: physiology and pathobiology. *J Am Coll Cardiol* 2013;**62**:D22–33.
2. de Amorim Correa R, de Oliveira FB, Barbosa MM, Barbosa JA, Carvalho TS, Barreto MC *et al.* Left ventricular function in patients with pulmonary arterial hypertension: the role of two-dimensional speckle tracking strain. *Echocardiography* 2016;**33**:1326–34.
3. Kishiki K, Singh A, Narang A, Gomberg-Maitland M, Goyal N, Maffessanti F *et al.* Impact of severe pulmonary arterial hypertension on the left heart and prognostic implications. *J Am Soc Echocardiogr* 2019;**32**:1128–37.
4. Padervinskienė L, Krivickienė A, Hoppenot D, Miliauskas S, Basevičius A, Nedzelskienė I *et al.* Prognostic value of left ventricular function and mechanics in pulmonary hypertension: a pilot cardiovascular magnetic resonance feature tracking study. *Medicina (Kaunas)* 2019;**55**:73.
5. Pedrizzetti G, La Canna G, Alfieri O, Tonti G. The vortex–an early predictor of cardiovascular outcome? *Nat Rev Cardiol* 2014;**11**:545–53.
6. Guerra M, Amorim MJ, Bras-Silva C, Leite-Moreira AF. Intraventricular pressure gradients throughout the cardiac cycle: effects of ischaemia and modulation by afterload. *Exp Physiol* 2013;**98**:149–60.
7. Guerra M, Bras-Silva C, Amorim MJ, Moura C, Bastos P, Leite-Moreira AF. Intraventricular pressure gradients in heart failure. *Physiol Res* 2013;**62**:479–87.
8. Firstenberg MS, Smedira NG, Greenberg NL, Prior DL, McCarthy PM, Garcia MJ *et al.* Relationship between early diastolic intraventricular pressure gradients, an index of elastic recoil, and improvements in systolic and diastolic function. *Circulation* 2001;**104**:I330–5.
9. Pedrizzetti G. On the computation of hemodynamic forces in the heart chambers. *J Biomech* 2019;**95**:109323.
10. Lapinskas T, Pedrizzetti G, Stoiber L, Dungen HD, Edelmann F, Pieske B *et al.* The intraventricular hemodynamic forces estimated using routine CMR cine images: a new marker of the failing heart. *JACC Cardiovasc Imaging* 2019;**12**:377–9.
11. Pedrizzetti G, Claus P, Kilner PJ, Nagel E. Principles of cardiovascular magnetic resonance feature tracking and echocardiographic speckle tracking for informed clinical use. *J Cardiovasc Magn Reson* 2016;**18**:51.
12. Chamsi-Pasha MA, Zhan Y, Debs D, Shah DJ. CMR in the evaluation of diastolic dysfunction and phenotyping of HFpEF: current role and future perspectives. *JACC Cardiovasc Imaging* 2020;**13**:283–96.
13. Driessen MMP, Schings MA, Sieswerda GT, Doevendans PA, Hulzebos EH, Post MC *et al.* Tricuspid flow and regurgitation in congenital heart disease and pulmonary hypertension: comparison of 4D flow cardiovascular magnetic resonance and echocardiography. *J Cardiovasc Magn Reson* 2018;**20**:5.
14. Galie N, Humbert M, Vachiery JL, Gibbs S, Lang I, Torbicki A *et al.*; ESC Scientific Document Group. 2015 ESC/ERS Guidelines for the diagnosis and treatment of pulmonary hypertension: the Joint Task Force for the Diagnosis and Treatment of Pulmonary Hypertension of the European Society of Cardiology (ESC) and the European Respiratory Society (ERS): endorsed by: association for European Paediatric and Congenital Cardiology (AEPC), International Society for Heart and Lung Transplantation (ISHLT). *Eur Heart J* 2016;**37**:67–119.
15. Nagueh SF, Smiseth OA, Appleton CP, Byrd BF III, Dokainish H, Edvardsen T *et al.* Recommendations for the evaluation of left ventricular diastolic function by echocardiography: an update from the American Society of Echocardiography and the European Association of Cardiovascular Imaging. *J Am Soc Echocardiogr* 2016;**29**:277–314.
16. Rudski LG, Lai WW, Afilalo J, Hua L, Handschumacher MD, Chandrasekaran K *et al.* Guidelines for the echocardiographic assessment of the right heart in adults: a report from the American Society of Echocardiography endorsed by the European Association of Echocardiography, a registered branch of the European Society of Cardiology, and the Canadian Society of Echocardiography. *J Am Soc Echocardiogr* 2010;**23**:685–713; quiz 86–8.
17. Tello K, Axmann J, Ghofrani HA, Naeije R, Narcin N, Rieth A *et al.* Relevance of the TAPSE/PASP ratio in pulmonary arterial hypertension. *Int J Cardiol* 2018;**266**:229–35.
18. Johns CS, Wild JM, Rajaram S, Tubman E, Capener D, Elliot C *et al.* Identifying at-risk patients with combined pre- and postcapillary pulmonary hypertension using interventricular septal angle at cardiac MRI. *Radiology* 2018;**289**:61–8.
19. Swift AJ, Rajaram S, Hurdman J, Hill C, Davies C, Sproson TW *et al.* Noninvasive estimation of PA pressure, flow, and resistance with CMR imaging: derivation and prospective validation study from the ASPIRE registry. *JACC Cardiovasc Imaging* 2013;**6**:1036–47.
20. Leng S, Tan RS, Zhao X, Allen JC, Koh AS, Zhong L. Validation of a rapid semi-automated method to assess left atrial longitudinal phasic strains on cine cardiovascular magnetic resonance imaging. *J Cardiovasc Magn Reson* 2018;**20**:71.
21. Mitter SS, Shah SJ, Thomas JD. A test in context: E/A and E/e' to assess diastolic dysfunction and LV filling pressure. *J Am Coll Cardiol* 2017;**69**:1451–64.
22. Sjögren H, Kjellström B, Bredfelt A, Steding-Ehrenborg K, Rådegran G, Hesselstrand R *et al.* Underfilling decreases left ventricular function in pulmonary arterial hypertension. *Int J Cardiovasc Imaging* 2021;**37**:1745–55.
23. Lin ACW, Seale H, Hamilton-Craig C, Morris NR, Strugnell W. Quantification of biventricular strain and assessment of ventriculo-ventricular interaction in pulmonary arterial hypertension using exercise cardiac magnetic resonance imaging and myocardial feature tracking. *J Magn Reson Imaging* 2019;**49**:1427–36.
24. Haddad F, Hunt SA, Rosenthal DN, Murphy DJ. Right ventricular function in cardiovascular disease, part I: anatomy, physiology, aging, and functional assessment of the right ventricle. *Circulation* 2008;**117**:1436–48.
25. Tsang TS, Barnes ME, Gersh BJ, Bailey KR, Seward JB. Left atrial volume as a morphophysiologic expression of left ventricular diastolic dysfunction and relation to cardiovascular risk burden. *Am J Cardiol* 2002;**90**:1284–9.
26. Kasner M, Westermann D, Steendijk P, Dröse S, Poller W, Schultheiss HP *et al.* Left ventricular dysfunction induced by nonsevere idiopathic pulmonary arterial hypertension: a pressure-volume relationship study. *Am J Respir Crit Care Med* 2012;**186**:181–9.
27. Gurudevan SV, Malouf PJ, Auger WR, Waltman TJ, Madani M, Raisinghani AB *et al.* Abnormal left ventricular diastolic filling in chronic thromboembolic pulmonary hypertension: true diastolic dysfunction or left ventricular underfilling? *J Am Coll Cardiol* 2007;**49**:1334–9.
28. Pedrizzetti G, Arvidsson PM, Toger J, Borgquist R, Domenichini F, Arheden H *et al.* On estimating intraventricular hemodynamic forces from endocardial dynamics: a comparative study with 4D flow MRI. *J Biomech* 2017;**60**:203–10.
29. Fadel E, Mercier O, Mussot S, Leroy-Ladurie F, Cerrina J, Chapelier A *et al.* Long-term outcome of double-lung and heart-lung transplantation for pulmonary hypertension: a comparative retrospective study of 219 patients. *Eur J Cardiothorac Surg* 2010;**38**:277–84.